

## A New Method for the Evaluation of Wear Damage in Dry Rolling Contact by Sound Intensity Level and Residual Stress Measurements

J.T.N. Medeiros<sup>1</sup>, L.G.Martinez<sup>2</sup>, R.M.Souza<sup>3</sup>, D.K.Tanaka<sup>3</sup>

<sup>1</sup> Mech. Eng. Dept. - Federal Univ. of Rio G. Norte –Natal –RN–Brazil – [jtelesforo@yahoo.com](mailto:jtelesforo@yahoo.com)

<sup>2</sup> Energetic and Nuclear Research Institute –São Paulo–SP–Brazil– [lgallego@net.ipen.br](mailto:lgallego@net.ipen.br)

<sup>3</sup> Polytechnic School of the Univ. of São Paulo – Surface Phenomena Laboratory – São Paulo–SP–Brazil - [roberto.souza@poli.usp.br](mailto:roberto.souza@poli.usp.br), [dktanaka@usp.br](mailto:dktanaka@usp.br)

**Key-words:** Wear; Residual Stresses; Noise; Rolling Contact Fatigue, XRD, Tribology.

**Abstract.** The contact fatigue wear of rolling surfaces is associated with the behavior of dislocations located at the specimen surface and subsurface. This behavior depends on the Hertzian Pressure and specimen shear strength, which affect the residual stress fields developed during cyclic loading. This work describes a new nondestructive method to evaluate changes on the residual stress fields and wear damage in dry rolling contact. A disc-disc testing machine was used into a semi-anechoic chamber to evaluate the audible sound signal (noise intensity level) continuously generated by the mechanical contact. Pairs of discs of heat treated DIN 100Cr6 (AISI 52100) steel were tested under Hertzian nominal pressures from  $P_0 = 1.5$  GPa to  $P_0 = 2.5$  GPa, at velocities of  $40 \pm 0.5$  m/s. The sound signals were later distributed into box-and-plot graphics which indicated four percentile groups (quartiles) and revealed the main tendency and dispersion of these signals. An XRD analysis, using the  $\sin^2\psi$  technique was applied to measure the residual stresses and to associate them with the noise intensity level quartiles at different stages of testing. Microstructural analyses of tested disc surfaces and resulting debris, using a Scanning Electron Microscope (SEM), showed a relation between the different noise levels and surface damage mechanisms, such as microspalling, micropitting, plastic deformation, delamination and brittle fracture.

### Introduction

Cyclic wear damages that occur on rolling bearings, cam-followers, gears and wheel-rail can lead to catastrophic failures such as the one shown in Fig. 1.

Wear under cyclic loading involves fracture near the surface and delamination of material due to plastic deformation [1]. During this process, plastic flow occurs at the surface region, controlled by the contact history and stress concentration parameters, while the inner subsurface part behaves elastically. The interaction between these two zones generates compressive macro and microstresses as a material response [2, 3, 4, 5, 6]. Particle detachment, resulting from delamination, leads to third body formation [7].

Around the contact zone, there is an aerodynamic flow of air.

This flow, associated with the nature of surfaces and real time local damages, produces a response to the local sound pressure. The use of acoustic techniques in monitoring of wear have been described [8, 9]. The Sound Pressure Level (SPL) response, although constituted by a signal which has a limited frequency band, generally up to 8 kHz (the sound is audible up to 20 kHz), is a real time tool that can be effective in revealing information about the rolling contact damage evolution. In addition to the acoustic techniques, the cyclically affected cross sections of the material contact

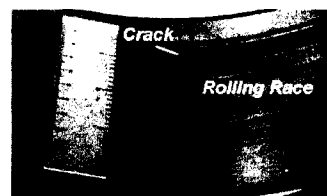


**Figure 1** – Catastrophic failure in a massive roller rolling bearing race

zone produce modifications on the residual stress state ( $\sigma_R$ ), which can be evaluated only after stopping of the structural members.

The aim of this investigation is to present a new approach that associates rolling wear mechanisms of a pair of discs to the SPL, to the number of cycles or rolling distance and to the residual stresses at the contact surface.

## Experimental Procedure

### Rolling Contact Setup, Sound Pressure Level (SPL) and Residual Stress ( $\sigma_R$ ) Measurements

A PLINT TE73 disc-disc testing machine was used during the wear tests. Six DIN 100Cr6 (AISI 52100) steel discs were heat treated to provide a predominantly martensitic microstructure. Previous set of experiments involved pairs of this same batch of DIN 100Cr6 steel discs [10], together with a Nitrided Cast Iron-Nitrided Cast Iron pair [11] and a Steel-Copper pair [12]. In terms of the Six DIN 100Cr6 steel discs, the nominal range of Hertzian pressures and velocities used were 1.54 to 2.49 GPa and  $40.0 \pm 0.5$  m/s, respectively. Table 1 and Fig. 2 present material and geometrical parameters of the discs at which residual stresses were measured. Profile grinding provided a spherical race surface for the contact zone.

**Table 1.** Geometrical characteristics for races of the three pairs of steel discs

Disc	Race Radius [mm]		Surface Roughness [ $\mu\text{m}$ ]				Race <sup>(*)</sup>		Precrack [ fig. 2(e) ]		
	R <sub>axial</sub>	R <sub>circun</sub>	Ra <sub>axial</sub>	Ra <sub>circun</sub>	Thickness[mm]						
Driver 1, 2, 3	75.00±2.0	75.00±0.05	0.44	0.14	8.150		No				
Driven 1	75.00±2.0	76.00±0.05	0.43	0.18	8.150		Yes				
Driven 2, 3	75.00±2.0	75.00±0.05	0.43	0.14	8.150		No				
	C	Ni	Mn	Cr	P	Cu	S	Ti	Si	V	HRC
% mass	1.00	0.030	0.380	1.46	0.016	0.009	0.015	0.006	0.270	0.005	65±1.5

During the wear tests, the SPL (Sound Pressure Level) was continuously measured by a Sound Pressure Meter, located at a horizontal distance 0.80 m far from and perpendicular to the contact tangential plane. The SPL meter operated in a frequency range from 20 Hz to 8 KHz, in a dB range from 40 to 130 dB and with a 0.1 dB resolution and  $\pm 1.6$  % precision. This meter was connected to a data acquisition system and a SPL acquisition frequency of 1 Hz was adopted to continuously monitor the evolution of the wear by acoustic signal. The testing machine was also connected to an automatic stopping sensor, which stopped the experiment when the vibration amplitude reached a fixed value. When this limit was set at two pre-determined values, it was possible identify three different wear conditions for the contact:  $L_0$ , the initial condition ("new" surface, after surface treatment and profile grinding);  $L_1$ , a moderate or oxidative wear condition and  $L_2$ , a contact fatigue wear condition, where subsurface cracks were propagating towards the surface.

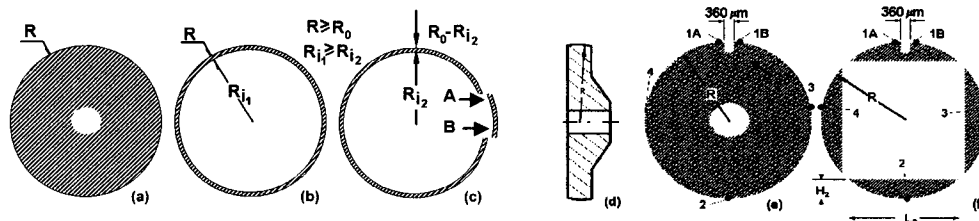


**Figure 2.** Testing disc configurations used to measure the residual stress state

Residual stress states were measured by the X-Ray Diffraction method and the  $\sin^2\psi$  technique, using positive and negative  $\psi$  values of  $0^\circ$ ,  $\pm 15^\circ$ ,  $\pm 30^\circ$ ,  $\pm 45^\circ$ . X-Ray diffraction measurements were performed in a RIGAKU D-MAX2000 diffractometer with its module *Stress*. It was used a

parallel beam geometry, scintillation detector, Cr-K $\alpha$  radiation ( $\lambda = 0.22910$  nm), without monochromator, 40 KV and 20 mA. The  $\sigma_R$  values measured for steel refer to reflection of the martensite (hkl) = 211), with peak at  $2\theta \approx 154.250^\circ$ . The  $2\theta$  angles covered were in the range  $148.0^\circ \leq 2\theta \leq 157.7^\circ$ , with  $0.1^\circ$  step. The assumed values of Young's Modulus and Poisson ratio were, respectively,  $E_{\text{Steel}211} = 215.75$  GPa and  $\nu = 0.300$ .

## Results and discussion

The wear damage evolution of the discs races can be observed by the residual stress data presented on Table 2 and on the graphs of the means and measurement reliability of the residual stress states shown in Fig. 3. These data are relative to pairs of discs with initial configurations presented in Fig. 2(a) and 2(e).

**Table 2.** Residual Stress Measurement in the DIN 100Cr6 Steel Races

DISC	Steel-Steel Testing			$\sigma_R(+)$		$\sigma_R(-)$		$\sigma_R$		$P_{\text{Hertz}}/\sigma_R$ Relation [**]
	Load [KN]	$P_{\text{Hertz}}$ [GPa]	RD: Km (Mcycl)	Mean [GPa]	Dev. GPa(+)	Mean [GPa]	Dev. GPa(+)	Mean [GPa]	Dev. GPa(+)	
NEW	-	-	-	-0.24	0.02	-0.06	0.02	-0.15	0.02	-
DrivenC1 <sup>(1)</sup> (Cycl1)	6.0 to	2.22 to	1,139	-1.58	0.22	-1.14	0.15	-1.36	0.19	1.7
DriverC1 <sup>(1)</sup> (Cycl1)	7.4	2.39	(2.42)	-1.09	0.05	-1.01	0.02	-1.05	0.04	2.2
(80) DrivenC2 <sup>(1)</sup>				-1.42	0.17	-1.18	0.24	-1.30	0.21	1.9
(80) DriverC2 <sup>(1)</sup>	7.0	2.35	1,881	-1.24	0.06	-1.18	0.00	-1.21	0.04	2.0
DrivenC2 <sup>(2)</sup> ring	to	to	(3.99)	-1.53	0.22	-1.25	0.18	-1.39	0.20	1.7
DrivenC2 <sup>(3)</sup> C ring	8.4	2.49		-1.45	0.17	-1.24	0.22	-1.34	0.20	1.8
DrivenC2 <sup>(3)</sup> AB ring				-1.22	0.17	-1.19	0.07	-1.21	0.13	2.0
NEW	-	-	-	-0.08	0.03	-0.01	0.05	-0.04	0.04	-
(88)Driver-1A-C1 <sup>(4)</sup>				-0.79	0.03	-0.63	0.03	-0.71	0.03	3.0
Driver-2-C1 <sup>(4)</sup>	5.0	2.08	1,216	-0.95	0.06	-0.78	0.07	-0.87	0.06	2.5
Driver-3-C1 <sup>(4)</sup>	to	to	(2.56)	-1.11	0.05	-0.92	0.04	-1.01	0.05	2.1
Driver-4-C1 <sup>(4)</sup>	6.0	2.21		-0.87	0.04	-0.71	0.05	-0.79	0.05	2.7
DriverC2 <sup>(4)</sup>				-1.15	0.06	-1.13	0.08	-1.14	0.07	2.0
(88)Driven-1A-C2 <sup>(4)</sup>				-1.20	0.22	-1.15	0.09	-1.18	0.16	1.9
Driven-1B-C2 <sup>(4)</sup>				-1.36	0.08	-1.29	0.07	-1.33	0.08	1.7
Driven-2-C2 <sup>(4)</sup>	5.8	2.19	1,912	-1.06	0.18	-0.95	0.08	-1.01	0.14	2.3
Driven-3-C2 <sup>(4)</sup>	to	to	(4.03)	-1.22	0.17	-1.11	0.01	-1.17	0.12	1.9
Driven-4-C2 <sup>(4)</sup>	7.2	2.35		-1.20	0.25	-1.10	0.03	-1.15	0.18	2.0
Driven-1A-C2 Hub Cap <sup>(5)</sup>				-1.04	0.11	-0.90	0.02	-0.97	0.08	2.3
Driven-1B-C2 Hub Cap <sup>(5)</sup>				-1.12	0.20	-0.90	0.00	-1.01	0.14	2.2
(89)Driver <sup>(1)</sup>	2.0 to	1.54 to	1,166	-1.29	0.09	-1.14	0.04	-1.21	0.07	1.4
	3.3	1.82	(2.47)							

(1) See Fig. 2(a) (3) See Fig. 2(c) (5) See Fig. 3 (b) RD=Rolling Distance, km (MegaCycles)

(2) See Fig. 2(b) (4) See Fig. 3(a) [\*\*] ( $P_{\text{Hertz}}/\sigma_R$ ) Statistics: Median = 2.0 ; Mean=2.1; S.d. = 0.38

Statistic data and analysis concerning to three SPL [dB] temporal windows (each window with 20 minutes and 1,200 points record) are presented in Table 3 and Fig. 4. These data are relative to the beginning of a rolling contact test ( $L_0$ : running-in), to 20 minutes before the first stopping ( $L_1$ : 1,216 km) and to the last 20 minutes before the second stopping ( $L_2$ : 1,912 km). Since the  $p$ -values = 0.0, the analysis of variance ( $\alpha = 1\%$ ) and Kruskal-Wallis test ( $\alpha = 5\%$ ) indicated that the three SPL data set means and medians are significantly different. Therefore, the used SPL technique was sensitive [10] to detect surface or subsurface changes at  $L_0$ ,  $L_1$ ,  $L_2$  life stages.

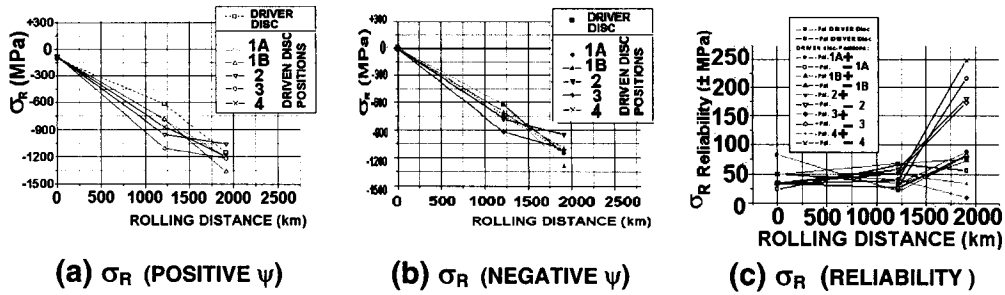


Figure 3 - Evolution of the Residual Stress according with the Rolling Distance at 40 m/s

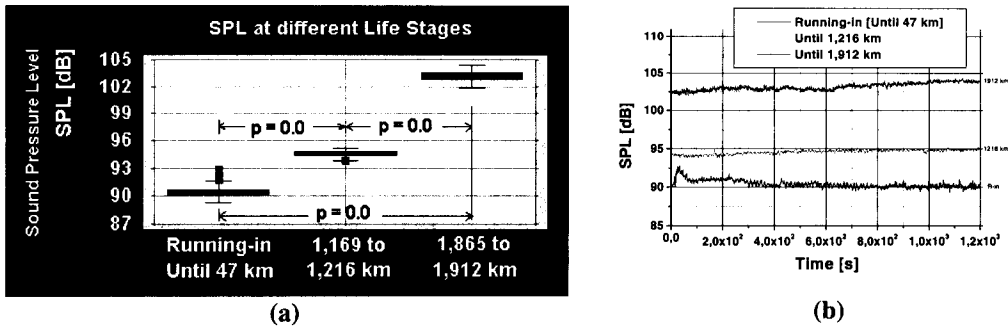


Figure 4. (a) Quartiles distribution of the SPL temporal signal around  $L_0, L_1, L_2$  life stages (*temporal quartil signatures*); (b) SPL temporal signal windows (*temporal analogic signatures*)

Table 3. Analysis of Variance on SPL [dB] for contact time windows (20 minutes) at running-in, at 1,216 km ( $2.56 \times 10^6$  cycles) and at 1,912 km ( $4.03 \times 10^6$  cycles)

Data	Mean [dB]	Variance	Standard Deviation	Median [dB]
Running-in	90.4	0.25	0.50 (0.6 %)	90.3
Until 1,216km	94.6	0.08	0.28 (0.3%)	94.7
Until 1,912km	103.2	0.26	0.51 (0.5%)	103.1

$F = 262451.46958$   $p = 0.0$   
 Test statistic (Kruskal-Wallis) = 3201.79  $p = 0.0$

At the 0.01 level, the means are significantly different (ANOVA)  
 At the 0.05 level, the medians are significantly different (Kruskal-Wallis)

In addition to the tabular form, SPL data *temporal signatures* are presented in Fig. 4(a) and 4(b). Initially, the 1,200 points of each window, corresponding to  $L_0, L_1, L_2$  life stages were distributed according quartiles and Fig. 4(a) simultaneously shows the mean, the median and *outliers* values, revealing all audible noise signal response behavior. Fig. 4(b) shows the conventional form of temporal SPL data presentation, where is quantitatively uncertain to obtain the central and dispersion tendencies. On the other hand, Fig. 4(b) is useful in providing information about localized contact events and its slope instantaneously reveals the SPL variation rate,  $\partial dB/\partial t$ , which is an indication of changes in the unlubricated rolling contact wear behavior.

The contact surface and subsurface zones constitute the track during cyclic rolling. In these zones, there is a superposition of the residual and Hertzian stresses fields and the tangential forces developed due to the friction and irreversibilities accumulated during the rolling process. Therefore, portions of the contact energy are spent to: (a) elastically deform the surface and subsurface zones; (b) plastically deform a thin layer parallel to the surface, when the yield limit of material is

overcame by the local stresses; (c) produce heat and/or mass transport; (d) support chemical reactions between and within contact surfaces.

During the cyclic rolling contact, slip occurs inside each grain and its neighbors of the contact zone, constituting the residual stress variations [2, 13]. The progressive cyclic rolling led to contact damage [3, 5], such as the occurrence of three-body abrasion, which is presented in Fig. 5. Such localized phenomena were identified by the residual stress measurements, which revealed a significant increase in the dispersion in the results (Fig. 3c).

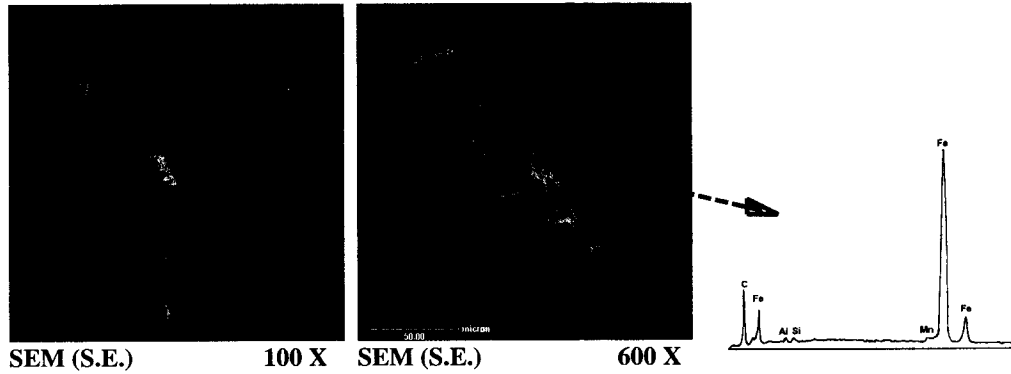


Figure 5. Track morphology of a tested surface revealing third body abrasion by carbide in the locus 3, as defined by Fig. 2(d). This phenomenon shows an increased dispersion of  $\sigma_R$ .

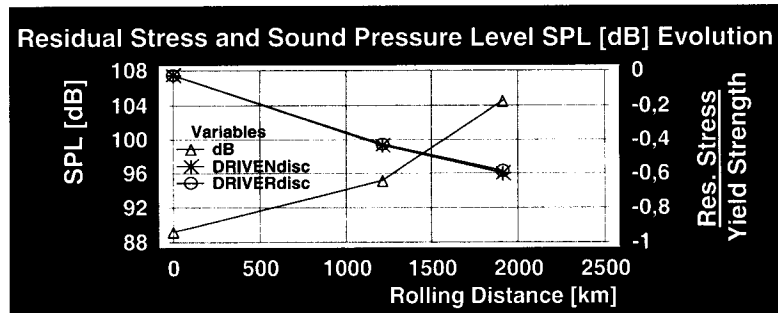


Figure 6 - Evolution of the Residual Stress and Sound Pressure Level versus the roling distance ( Yield Strength assumed as  $S_{y.s.} = 1.95$  GPa;  $S_{u.s.} = 2.00$  GPa )

Table 4. Overview of calibration models to Sound Pressure Level [ dB ] data until 1,912 km

Model	Correlation	R-Squared	Incercept (A) (p-value)	Slope (B) (p-value)	Mathematical Model
Reciprocal-Y	0.9494	90.13%	0.011167 (0.0000)	-7.02045x10 <sup>-7</sup> (0.0000)	dB=1/[A+B.(RD)]
Exponential	0.9443	89.17%	4.49362 (0.0000)	6.75895x10 <sup>-5</sup> (0.0000)	dB =exp[A+B.(RD)]
Square Root-Y	0.9417	88.67%	9.45451 (0.0000)	3.31782x10 <sup>-4</sup> (0.0000)	dB =[A+B.(RD)] <sup>2</sup> RD=rolling distance[km]

At a mesoscale, an irreversible portion of the contact energy increased the zone damaged by the cyclic contact, which affected  $\sigma_R$  [GPa] and Sound Pressure Level ( SPL [dB] ) values (Fig. 6 and Table 4). Therefore, both methods have their relevance: SPL temporal windows provide data for the

statistical moments of the rolling wear without operational interruption (Fig. 4, Table 3) and the statistical moments of  $\sigma_R$  reveal local phenomena (Fig. 3c, Table 2) in the races.

### Conclusions

Unlubricated races of grounded solid surfaces of DIN100Cr6 steel rolling were tested in a disc-disc rolling testing machine until 1,912 km. As measured by the experimental setup and under the described tests conditions, the results have shown that:

- 1) Residual stress variations,  $\sigma_R$  [GPa], as measured by X-ray diffraction,  $\sin^2\psi$  technique, and Sound Pressure Level temporal windows ( SPL [dB] ) were statistically significant according to a variation with the rolling distance;
- 2) While  $\sigma_R$  revealed wear local phenomena in the races, SPL showed, at real time, non-stopping, the rolling wear evolution;
- 3) After the first stopping (1,216 km), controlled by a vibration trip sensor, and until the second (1,912 km), the relation  $P_{\text{Hertz}} / \sigma_R$  had a variation between 1.4 and 3.0, having median 2.0, mean 2.1 and standard deviation of 0.38.

### Acknowledgements

The authors would like to thank the Coordination for High-level Manpower Education ( CAPES ) of the Brazilian Ministry of Education for the support of Ph.D. program of J. T. N. Medeiros.

### References

- [1.] N.P. Suh: *Wear*, Vol. 25 (1973), p. 111-124.
- [2.] F.A. McClintock: The mechanics of elastic-plastic fracture. In: F.A. McClintock and A.A. Argon: *Mechanical Behavior of Materials* (Addison-Wesley, Reading-MA, 1966), p. 534-540.
- [3.] D. Nélias, M.L. Dumont, F. Couhier, F.; G. Dudragne; L. Flamand: *ASME J. Trib.*, Vol.120 (1998), p. 184-190.
- [4.] I.C. Noyan and J.B. Cohen: *Residual Stress: Measurement by Diffraction and Interpretation* (Springer, Berlin 1987).
- [5.] A.P. Voskamp and E.J. Mittemeijer: *Zeitschrift fuer Metallkunde* Vol. 88 (4), 1997, p. 310-320.
- [6.] W.Weibull: Efficient Methods for Estimating Fatigue Life Distributions of Roller Bearings. In: J.B. Bidwell (ed.) *Rolling Contact Phenomena* (Elsevier, Amsterdam, 1962), p. 252-265.
- [7.] A. Benrabah, C. Langlade and A.B. Vannes: *Wear*, Vol. 224 (1999), p. 267-273.
- [8.] J. Miettinen and V. Siekkinen: *Wear*, Vol. 181-183 (1995), p. 897-900.
- [9.] C.G. Stanworth: *Wear*, Vol. 113 (1986), p. 143-150.
- [10.] J.T.N. Medeiros, A. Sinatora and D.K. Tanaka: Audible noise, contact temperature, life and microfracture of dry rolling surfaces using DIN100Cr6 Steel. In: Portuguese Society of Materials, *Proc of the First International Materials Symposium.*. Coimbra, University of Coimbra, 2001, paper MatLif10.
- [11.] C.R.F. Hernandez, F.U. Ordoñez, J.T.N. Medeiros, A.M. Oliveira, A. Sinatora and D.K. Tanaka: Rolling Contact Fatigue Wear of Nitriding Austempered Ductile Iron (ADI)-ADI Steels. In: *Proc. (CD-rom) of Brazilian Congress of Mechanical Engineering., COBEM-2001*, Federal University of Uberlândia.
- [12.] J.T.N. Medeiros, L.G. Martinez, R.M. Souza and D.K. Tanaka: Evolução de tensões residuais em discos desgastados por rolamento cíclico não lubrificado. In: *Proc. (CD-rom) of CONEM 2002 - National Congress of Mechanical Engineering.* João Pessoa, UFPb, 2002. (in portuguese).
- [13.] A.P. Voskamp: *Mater. Sci. Forum*, Vol. 347-349 (2000), p.346-351.

## **Residual Stresses VI, ECRS6**

doi:10.4028/www.scientific.net/MSF.404-407

## **A New Method for the Evaluation of Wear Damage in Dry Rolling Contact by Sound Intensity Level and Residual Stress Measurements**

doi:10.4028/www.scientific.net/MSF.404-407.773